

## **Porphyrins 42\*. Ground and Excited State Calculations on the Isomers of Free Base Porphine and Sirohydrochlorin**

Diane C. Rawlings, Ernest R. Davidson, and Martin Gouterman

Department of Chemistry, University of Washington, Seattle, WA 98195, USA

Symmetry instabilities were encountered during MINDO/3 geometry optimizations of the sirohydrochlorin and porphine isomers leading to bond alternating optimal structures. Transition energies and oscillator strengths were calculated with INDO/S/CI. Our calculations predict the ground state *cis* and *trans* isomers of sirohydrochlorin to be close in energy and confirm the experimental assignment of the absorptions bands, with the *cis* tautomer having a red shifted spectrum.

**Key words:** Sirohydrochlorin – Isobacteriochlorin – Porphine – Porphyrins – MINDO/3 – INDO/S/CI.

Sirohydrochlorin (Fig. 1) has been found to be an intermediate in the biosynthesis of vitamin B<sub>12</sub> [1, 2, 3]. It is also a demetallated siroheme. Siroheme is the prosthetic group in two enzymes which catalyze the six electron reduction of sulfite to hydrogen sulfide and nitrite to ammonia [4, 5].

Chang has reported optical and IR absorption spectra at various temperatures on model sirohydrochlorins [6]. These spectra show two species, which are ascribed to tautomers of the central protons. There is a “red” tautomer, with its longest wavelength optical absorption at 635 nm (2.0 eV), and an “orange” tautomer with its longest wavelength absorption at 588 nm (2.1 eV). Chang showed that the “red” tautomer disappears at low temperature. The existence of two tautomers has found further support by the study of the emission and

\* Part 41. Gouterman, M., Sayer, P., Shankland, E., Smith, J. P.: *Inorg. Chem.* **20**, 87 (1981)  
*Offprint requests and correspondence to:* D. C. Rawlings

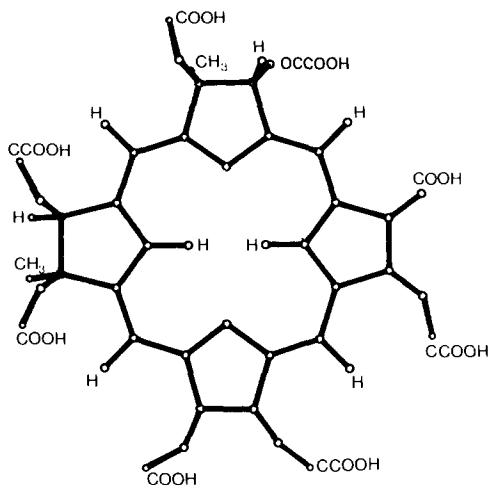


**Fig. 1.** Sirohydrochlorin (a demetallated siroheme), trans tautomer

excitation spectra of Chang's model sirohydrochlorins [6]. These studies show that (at room temperature) excitation into the "red" tautomer gave fluorescence with the shortest wavelength at 640 nm (1.9 eV); excitation into the "orange" tautomer (at room temperature) produces emission with the shortest wavelength at 590 nm (2.1 eV) plus emission from the "red" tautomer. Thus the low temperature absorption spectrum of Chang and the excitation spectrum at 590 nm gives the spectrum of the "orange" tautomer. The room temperature absorption spectrum and the excitation spectrum at approximately 640 nm gives a mixture of both species. Thus the full spectrum of the "orange" tautomer is well known. However, the experimental work is, as yet, insufficient to know accurately the ratios of the principal peaks of the "red" tautomer. Based on both absorption and emission spectra the peaks for the individual tautomers are shown in Fig. 2.

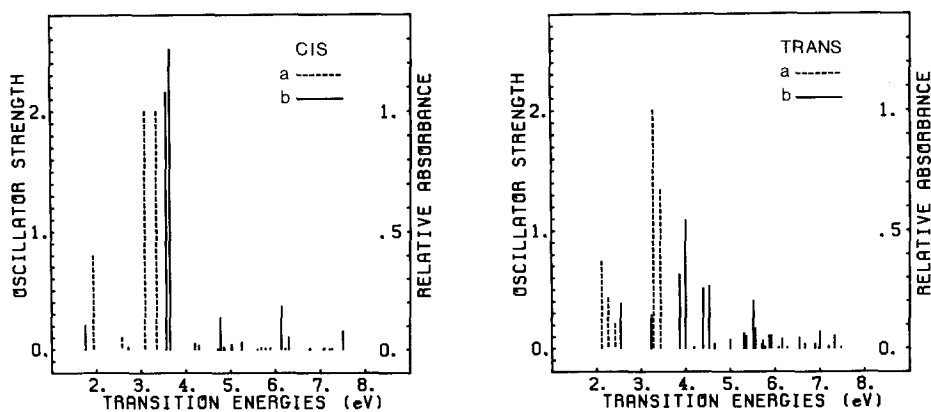


**Fig. 2.** **a** Relative absorbance maxima of the cis and trans tautomers of model sirohydrochlorin deduced from absorption and excitation spectra. The spectrum of the trans tautomer is well known. The intensity ratios for the cis tautomer are poorly known. **b** INDO/S calculated transitions at the cis  $C_{2v}$  optimal geometry and the trans unconstrained optimal geometry

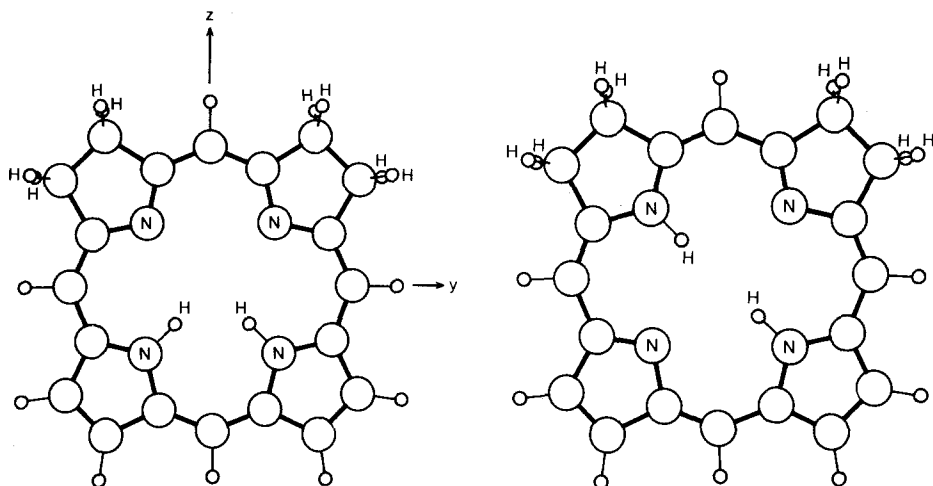


Fig. 3. cis and trans model sirohydrochlorins

Based on qualitative reasoning, Chang deduced that the trans tautomer was likely to be more stable. Furthermore, he found evidence in the IR spectra to support this view. A principal reason for having undertaken the present calculations was to see if theoretical calculations would predict the more stable tautomer and whether one tautomer is indeed "red" and the other "orange." It will be seen that our conclusions match those of Chang, so henceforth we refer to the "red" tautomer as cis and the "orange" tautomer as trans.

In  $D_{4h}$  porphyrins the  $B$ (Soret) and  $Q$  bands are ( $\pi \rightarrow \pi^*$ ) absorptions involving a linear combination of excitations from the two highest occupied molecular orbitals (HOMO's) into the two lowest unoccupied MOs (LUMO's) according to the four orbital model [7]. In  $D_{4h}$  these are  $a_{1u}, a_{2u} \rightarrow e_g$  excitations. The  $Q$

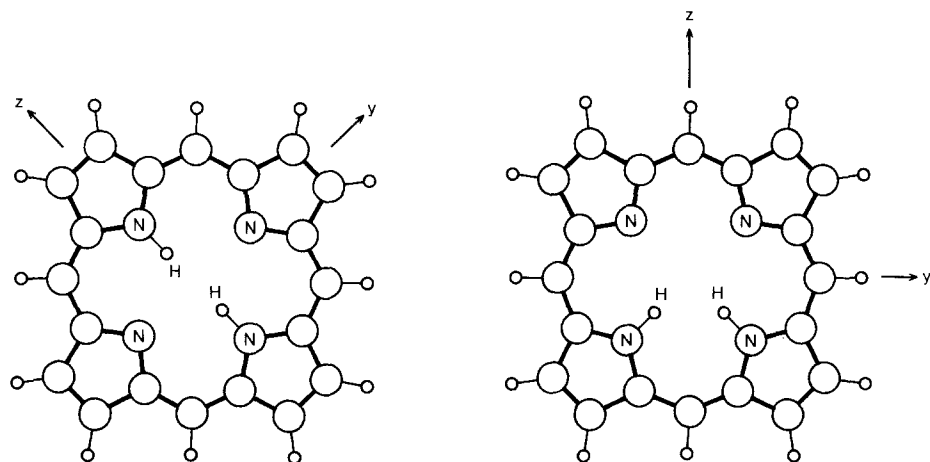
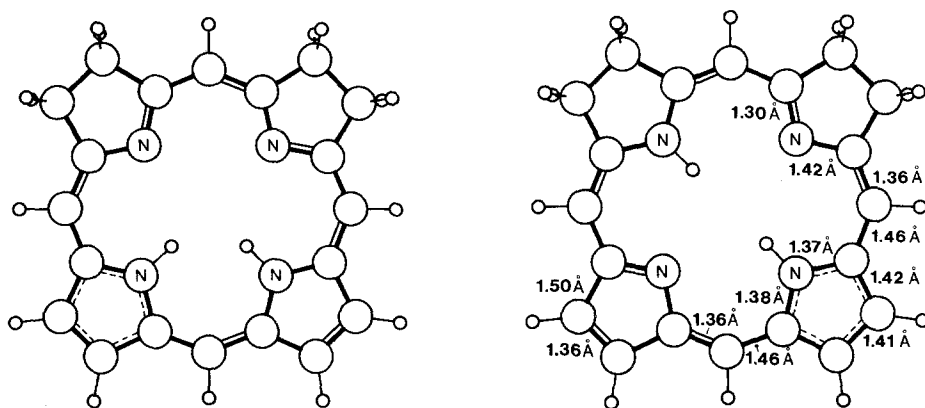


Fig. 4. cis and trans porphine

and  $B$  bands are split in free base porphyrins due to the lowered symmetry and splitting of the  $e_g$  orbitals. We have done MINDO/3 [8] ground state geometry optimizations on the cis and trans isomers of a model sirohydrochlorin (Fig. 3) in an attempt to determine appropriate model sirohydrochlorin geometries and an approximate ground state energy difference between the tautomers. Using unoptimized and various optimal MINDO/3 geometries, we calculated excited states and transition moments for each isomer using an INDO/S/CI program. As a comparison and test of the method we applied the same procedure to the much studied porphine isomers (Fig. 4).

### MINDO/3 Geometry Optimizations of Sirohydrochlorin and Porphine: Examples of Bond Alternation and Symmetry Instabilities

At the time these calculations were done, X-ray structures for sirohydrochlorin were not known. X-ray determination of the structure of a model sirohydrochlorin [9] has recently been completed and its implications are discussed later. However, X-ray geometries are known for porphine and the trans tautomer is confidently thought to be the isomer present at room temperature [10, 11]. For this reason we used porphine as an indicator of the believability of our MINDO/3 results. Unconstrained geometry optimizations of the two model sirohydrochlorin tautomers produced wavefunctions and geometries of broken symmetry. In particular, these optimizations produced bond alternation around the macrocycle (Fig. 5). We completed two different unconstrained optimizations for each tautomer, once beginning from a  $C_{2v}$  geometry averaged over the X-ray structure of ZnTPiBC (Zinc tetraphenylisobacteriochlorin) [12] and once beginning with the ZnTPiBC X-ray structure ( $C_s$  symmetry). At the initial  $C_{2v}$  geometry the cis sirohydrochlorin wavefunction (as indicated from the pi electron density) maintains  $C_{2v}$  symmetry. However, the pi bond orders alternate where the assumed bond lengths do not (see Fig. 6). The trans tautomer at the same initial " $C_{2v}$ "



**Fig. 5.** Unconstrained optimal geometries of the model cis and trans tautomers of sirohydrochlorin showing bond alternation. Double bonds are indicated by two bond lines. Dashed lines indicate localized resonant structures

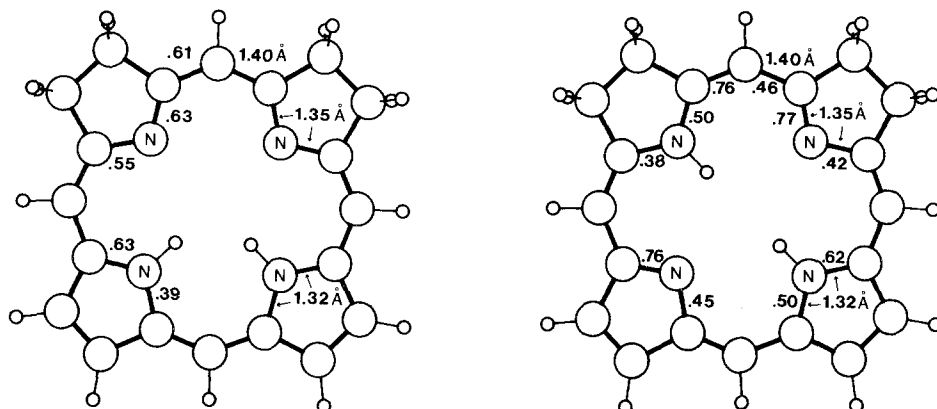


**Fig. 6.** Selected bond lengths and calculated pi bond orders at the initial " $C_{2v}$ " geometries for the sirohydrochlorin tautomers

ring geometry but with the interior hydrogens on opposite nitrogens ( $C_s$  symmetry overall) shows bond order alternation around the macrocycle except in one pyrrole ring where the bond orders indicate a resonant structure (see Fig. 6). The unconstrained optimizations involved the simultaneous optimization of 126 parameters. The unconstrained optimal ground state energies are reported in Table 1. Within the accuracy of these calculations the cis and trans tautomers have the same ground state energies.

**Table 1.** MINDO ground state energies for the sirohydrochlorin and porphine isomers

Molecule	Geometry	$H_{f298}(\text{kJ/mol})$
cis sirohydrochlorin	unconstrained optimal	418 <sup>a</sup>
	initial $C_{2v}$ <sup>b</sup>	754
	optimal $C_{2v}$	452
	X-ray ( $C_s$ symmetry) <sup>b</sup>	812
trans sirohydrochlorin	unconstrained optimal	420 <sup>a</sup>
	initial approx. $C_{2v}$ <sup>b</sup>	749
	optimal approx. $C_{2v}$	427
cis porphine	unconstrained optimal	703
	optimal $C_{2v}$	754
	averaged X-ray ( $C_{2v}$ ) <sup>c</sup>	917
trans porphine	optimal unconstrained	695
	optimal $D_{2h}$	745
	averaged X-ray <sup>c</sup>	888

<sup>a</sup> cis tautomer is lower than the trans by 2.1 kJ/mol

<sup>b</sup> Initial geometries from ZnTPiBc X-ray structure averaged for  $C_{2v}$  geometry

<sup>c</sup> Ref. [10]

MINDO/3 is known to predict bond alternating structures in the higher numbered annulenes [13], e.g. 18-annulene, which has been used as a model of the porphyrin macrocycle. At the SCF level the bond-alternating 18-annulene is more than 105 kJ/mol lower in energy than its aromatic partner [14]. However, after the inclusion of correlation effects by either CI or perturbation theory, the aromatic structure is lower in energy. The incorrect prediction of a lower symmetry form of a singlet, closed shell molecule by the SCF procedure is well known as the "singlet instability problem". Considering the MINDO/3 predictions for 18-annulene we must be skeptical of the MINDO/3 prediction of an alternating geometry for sirohydrochlorin. However, a recent X-ray structure of model sirohydrochlorins [9] does show evidence for some bond alternation. The bond alternation is in accord with an average of the predicted MINDO/3 geometries of the two possible trans arrangements of the interior hydrogens.

For a comparison we ran symmetry unconstrained optimizations on porphine. The initial geometry for the trans porphine isomer was taken from the averaged X-ray structure [10]. The initial geometry for the cis isomer was assumed to be a "cis" juxtaposition of the average X-ray pyrrole and pyrrolidine geometries in porphine. The wavefunctions at these initial points maintained the overall symmetries of the molecules, although the cis isomer showed some "local" (pyrrole) symmetry breaking, i.e. bond orders not corresponding to geometrical bond lengths (see Fig. 7). With an unconstrained geometry optimization (112 parameters) the wavefunctions and geometries did break symmetry and produced bond alternating structures. An optimization of the trans isomer constrained to maintain a  $D_{2h}$  geometry gave a  $D_{2h}$  wavefunction and a non-bond alternating geometry similar to the X-ray structure. We also optimized the cis isomer of porphine constrained to maintain a  $C_{2v}$  geometry. Although this constrained optimization showed no bond alternation, it did exhibit a first order symmetry instability, i.e. the optimal wavefunction (as indicated by the pi electron densities) does not have  $C_{2v}$  symmetry even though the geometry does. The trans isomer behaved nicely using a  $D_{2h}$  constrained optimization. However, because the cis isomer exhibits a first order symmetry instability the symmetry constrained

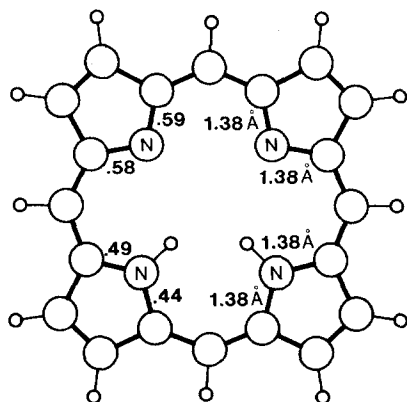


Fig. 7. Selected bond lengths and calculated pi bond densities for the initial  $C_{2v}$  geometry of the cis porphine isomer

cis–trans energy differences cannot be compared. It is possible that correlation effects will be larger for the cis isomer than for the trans. At least, the correlation effects are not comparable. Initial and optimal energies are reported in Table 1. At the initial averaged X-ray geometries the trans tautomer is lower in energy by 28.5 kJ/mol. At the unconstrained optimal geometries the trans is lower by 9.2 kJ/mol. Thus calculations at the X-ray and optimal geometries agree that the trans isomer of porphine is the more stable.

Given the apparent success in a constrained optimization of the trans porphine isomer, we reoptimized the cis sirohydrochlorin tautomer constraining the geometry to maintain  $C_{2v}$  symmetry (48 parameters). The resulting structure is bond alternating to some extent and corresponds closely to the wavefunction of broken “local” symmetry at the initial  $C_{2v}$  geometry (see Fig. 6). Without justification, we attempted to optimize approximately the same number of parameters (49) in a constrained calculation of the trans tautomer ( $C_s$  symmetry). This meant imposing not only the plane of the macrocycle but also a “partial” mirror plane along the interior N–H bonds excluding the parameters involving the hydrogen and four carbons which are not equivalent by symmetry across this plane. Again the constrained optimal geometry is bond-alternating to some extent and corresponds to the wavefunction of broken “local” symmetry at the initial trans geometry (see Fig. 6). The energies for these constrained optimizations for the cis and trans tautomers are listed in Table 1. The unconstrained optimal cis structure is 2.1 kJ/mol lower in energy than the unconstrained optimal trans structure. The constrained optimizations for the cis and trans tautomers are not comparable since the trans tautomer was artificially constrained.

We cannot conclude a definitive energy difference between the cis and trans isomers of either sirohydrochlorin or porphine from these MINDO/3 calculations because of the symmetry instability problems encountered. However, the sirohydrochlorin cis–trans energy difference is quite small (14.7 kJ/mol at the initial geometries and  $-2.1$  kJ/mol at the unconstrained optimal geometries) and confirms the possibility that the two species are actually tautomers at room temperature. The experimental sirohydrochlorin cis–trans energy difference determined on Chang’s compound is 5.4 kJ/mol [6]. The predicted porphine cis–trans energy difference ranges from 28.5 kJ/mol at the initial geometries to 9.2 kJ/mol at the unconstrained optimal geometries. Independent of the geometry used, trans porphine is predicted in these calculations to be more than  $kT$  higher in energy than the cis isomer (at 298 K).

### **INDO/S/CI Ground and Excited State Calculations to Predict the Spectra of the Model Sirohydrochlorin and Porphine**

We have computed the ground and excited states of the cis and trans isomers for sirohydrochlorin at various optimal geometries obtained from the MINDO/3 calculations described above and for the porphine isomers using the constrained optimal geometries obtained from MINDO/3. These calculations employed the Zerner INDO program [15] which has been parameterized to closely predict

the spectra of benzene and pyridine using ground state orbitals and a 45–55 dimensional CI composed of configurations singly excited from the ground state. It is possible to also include double excitations from the ground state. However, this procedure preferentially lowers the ground state energy because the corresponding double excitations from the excited state cannot be included. We report predicted spectra from single excitation calculations and also from calculations including single and double excitations. Although including a limited set of doubly excited configurations more closely reproduces experimental porphyrin spectra, we feel this procedure is not a justifiable one for calculating ground and excited state energy differences. However, we believe that the introduction of new states into the Soret region when double excitations are included may be qualitatively correct. Primary contributors to these states are doubly excited configurations within the four orbital model. The experimental consequences of such double excitations need to be explored.

Predicted transitions for the *cis* and *trans* tautomers are plotted in Fig. 2. Also see Table 2 for more detail and for a comparison of transitions at different geometries. As noted in previous porphyrin calculations, the geometry seems to make little qualitative difference for the lowest four transitions (see Table 2.1 and 2.3). However, there are some qualitative differences in the character of the higher energy electronic transitions at different macrocycle geometries, i.e., there are differences in the important configurations composing the CI vectors and quantitative differences in the predicted transition energies. The *cis* tautomer of sirohydrochlorin shows electronic transitions to the red of the *trans* tautomer by 0.74–0.84 eV, depending on the geometry and the number of single and double configurations included in the CIs. Thus our calculations clearly support Chang's *cis* and *trans* assignment of the *Q* and *B* absorption bands.

It is interesting to examine the molecular orbitals involved in the transition producing the *Q* and *B* (Soret) states. See Table 3 for molecular orbital symmetries and energies. The configurations contributing to the *Q* and *B* excited states are pi excitations primarily from the highest occupied  $a_2$  and  $b_1$  [ $a_{1u}$  and  $a_{2u}$  in  $D_{4h}$ ] orbitals into the lowest unoccupied  $a_2$  and  $b_1$  [ $e_g$  in  $D_{4h}$ ] orbitals. Although there are some differences in the contributions to these states in the *cis* and *trans* sirohydrochlorin tautomers, the major factor for the red shift of the *cis* tautomer is electrostatic. This can be seen by comparison of the *cis* and *trans* sirohydrochlorin molecular orbitals with those for siroberyllium, a sirohydrochlorin with a beryllium atom in the center of the macrocycle (BeiBC). Siroberyllium is a model of the sirohydrochlorin with a spherical +2 charge distribution in the center. The *cis* and *trans* positions of the hydrogens may be thought of as distortions of this spherical positive charge on the beryllium atom in the center of the macrocycle. Figure 8 shows the molecular orbital energy diagrams for the siroberyllium and the two sirohydrochlorin tautomers. The relative energies of the two highest occupied molecular orbitals and the two lowest unoccupied orbitals are of interest in examining the perturbation effect due to the placement of the interior hydrogens, i.e. the distortion of the positive charge in the center, on the *Q* and *B* states. The HOMO's and LUMO's in the



**Table 2.** Predicted transitions for the sirohydrochlorin tautomers

State	Contributing configurations	CI coefficients	Transition energies (eV)	Oscillator strengths
1. Cis sirohydrochlorin ( $C_{2v}$ optimal geometry; 43 configurations, singles only)				
1. $Q [B_2]$	59 → 60	0.8	1.76	0.21
	58 → 61	-0.5		
2. $Q [A_1]$	58 → 60	0.8	2.71	0.02
	59 → 61	0.6		
3. Soret [ $A_1$ ]	59 → 61	0.8	3.57	2.16
	58 → 60	-0.6		
4. Soret [ $B_2$ ]	58 → 61	0.8	3.65	2.52
	59 → 60	0.5		
5. [ $A_1$ ]	59 → 63	0.9	4.20	0.05
	58 → 62	0.4		
6. [ $B_2$ ]	59 → 62	0.8	4.29	0.03
7. $n \rightarrow \pi^*$ [ $B_1$ ]	55 → 61	0.9	4.72	0.03
8. [ $B_2$ ]	56 → 60	0.8	4.72	0.00
	54 → 60	0.4		
9. [ $A_1$ ]	57 → 60	0.8	4.77	0.00
10. [ $A_1$ ]	59 → 64	-0.7	4.85	0.02
	53 → 60	0.6		
Other transitions with relatively high oscillator strengths:				
20. [ $B_2$ ]	53 → 61	0.9	6.13	0.36
22 [ $A_1$ ]	54 → 61	0.7	6.30	0.10
	58 → 65	0.5		
2. Cis sirohydrochlorin ( $C_{2v}$ optimal geometry; 62 configurations, singles and selected doubles)				
State	Contributing configurations	CI coefficients	Transition energies (eV)	Oscillator strengths
1. $Q [B_2]$	59 → 60	0.8	1.79	0.23
	58 → 61	-0.5		
2. $Q [A_1]$	58 → 60	0.7	2.32	0.01
	59 → 61	0.6		
3. Soret [ $A_1$ ]	59 → 61	0.6	3.16	0.91
	58 → 60	-0.5		
	59 → 63	-0.4		
4. Soret [ $A_1$ ]	59, 59 → 60, 60	0.6	3.26	0.41
	59 → 61	0.4		
	59 → 63	0.4		
5. Soret [ $B_2$ ]	59 → 62	0.6	3.36	0.22
	59, 59 → 60, 61	-0.5		
	58 → 61	-0.4		
6. Soret [ $B_2$ ]	58 → 61	0.6	3.43	0.94
	58, 59 → 60, 60	-0.5		
7. [ $A_1$ ]	58, 59 → 60, 61	0.7	3.98	0.02
	58 → 62	0.5		

Table 2 (cont.)

8. [ $B_2$ ]	58→63	0.5	4.03	1.40
	56→60	-0.4		
	58→61	-0.4		
	58, 59→60, 60	-0.4		
9. [ $A_1$ ]	59→63	0.5	4.39	0.91
	57→60	-0.5		

## 3. Cis sirohydrochlorin (ZnTPiBc X-ray geometry; 43 configurations, singles only)

State	Contributing configurations	CI coefficients	Transition energies (eV)	Oscillator strengths
1. $Q$	59→60	0.9	1.74	0.25
	58→61	-0.5		
2. $Q$	58→60	0.8	2.77	0.01
	59→61	0.6		
3. Soret	59→61	0.8	3.52	1.92
	58→60	-0.6		
4. Soret	58→61	0.8	3.69	2.20
	59→60	0.5		
5.	59→62	0.9	4.08	0.01
6.	59→63	0.9	4.22	0.03
7.	56→60	0.6	4.73	0.03
	58→62	-0.5		
8.	57→60	0.8	4.80	0.15
9.	59→64	0.6	4.82	0.07
	55→61	-0.5		
10.	55→61	-0.7	4.87	0.02
	59→64	-0.4		

## 4. Trans sirohydrochlorin (unconstrained optimal geometry; 43 configurations, singles only)

State	Contributing configurations	CI coefficients	Transition energies (eV)	Oscillator strengths
1. $Q$	59→60	0.9	2.55	0.38
2. $Q$	59→61	0.9	3.23	0.28
3. Soret	58→60	0.8	3.87	0.63
	59→61	-0.4		
4. Soret	58→61	0.9	4.00	1.09
5. $n \rightarrow \pi^*$	53→60	1.0	4.19	0.01
	57→60	0.8		
6.	58→60	-0.4	4.39	0.51
	59→62	0.8		
7.	59→62	0.8	4.53	0.53
	59→63	-0.5		
8.	59→63	0.7	4.65	0.04
	59→62	0.5		
9.	56→60	0.7	5.00	0.07
	59→64	-0.4		
10.	58→62	0.7	5.31	0.13
	54→60	0.4		
	59→64	-0.4		

**Table 3.** Orbital numbers, symmetries and energies for the sirohydrochlorin tautomers<sup>a</sup>

Orbital number	Cis symmetry <sup>b</sup> designation	Cis orbital energies (eV)	Trans orbital energies (eV)
50	$a_2$	-11.89	-12.42
51	$b_1$	-10.94	-10.63
52	$a_1$	-9.97	-10.12
53	$b_1$	-9.79	-9.89
54	$a_2$	-9.76	-9.45
55	$b_2$	-9.63	-9.34
56	$a_2$	-9.18	-9.10
57	$b_1$	-8.99	-8.79
58	$b_1 [a_{2u}]$	-6.96	-7.63
59 HOMO	$a_2 [a_{1u}]$	-6.31	-6.47
60 LUMO	$b_1 [e_g]$	-1.50	-0.95
61	$a_2 [e_g]$	-0.63	0.54
62	$b_1$	0.86	0.86
63	$a_2$	0.90	0.96
64	$a_2$	1.69	1.86
65	$b_1$	2.29	2.11
66	$a_1$	2.29	2.14
67	$b_1$	2.51	2.32
68	$a_1$	2.54	2.69
69	$b_2$	2.55	2.69

<sup>a</sup> Cis tautomer at  $C_{2v}$  optimal geometry; trans at the unconstrained optimal geometry

<sup>b</sup>  $C_{2v}$  symmetry designations follow Mulliken convention with axes oriented as in Fig. 3

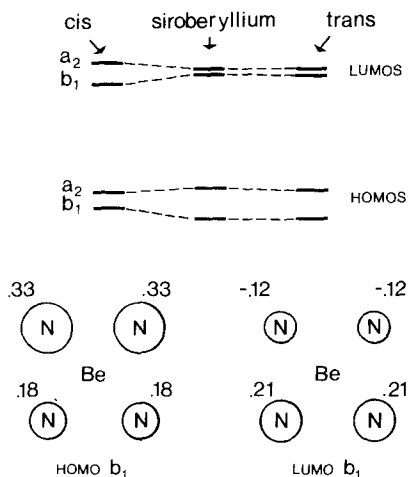


**Fig. 8.** Four orbital energy diagrams for the model sirohydrochlorins and for siroberyllium. Also shown are the MO coefficients on the nitrogens in the siroberyllium HOMO  $b_1$  and LUMO  $b_1$

**Table 4.** Predicted transitions for the porphine isomers

1. Cis porphine ( $C_{2v}$  geometry averaged from the X-ray structure; 65 configurations, singles only)

State	Contributing configurations	CI coefficients	Transition energies (eV)	Oscillator strengths
1. $Q [B_2]$	57→58	0.7	1.72	0.03
	56→59	-0.6		
2. $Q [A_1]$	57→59	-0.7	2.13	0.01
	56→58	-0.6		
3. Soret [ $B_2$ ]	56→59	-0.6	3.41	1.83
	57→58	-0.5		
	54→59	0.4		
4. Soret [ $A_1$ ]	56→58	0.6	3.47	1.89
	57→59	-0.6		
	55→59	-0.4		
5. [ $A_1$ ]	55→59	-0.6	3.81	0.62
	56→60	-0.5		
	56→58	-0.4		
6. [ $B_2$ ]	57→60	0.8	3.91	0.30
7. [ $B_2$ ]	55→58	0.5	4.12	0.85
	54→59	0.5		
8. [ $B_1$ ]	52→59	0.8	4.16	0.00
	52→58	-0.5		
9. [ $A_1$ ]	56→60	0.5	4.20	0.53
	55→59	-0.5		
	57→61	-0.5		
10. [ $A_2$ ]	52→58	-0.8	4.35	0.00
	52→59	-0.6		

2. Trans porphine ( $D_{2h}$  geometry averaged from the X-ray structure; 65 configurations, singles only)

State	Contributing configurations	CI coefficients	Transition energies (eV)	Oscillator strengths
1. $Q [B_{1u}]$	57→59	0.7	1.78	0.03
	56→58	-0.7		
2. $Q [B_{2u}]$	57→58	-0.8	2.08	0.09
	56→59	-0.6		
3. Soret [ $B_{1u}$ ]	56→58	-0.6	3.46	1.70
	57→59	-0.6		
	54→58	-0.5		
4. Soret [ $B_{2u}$ ]	56→59	0.7	3.65	2.12
	57→58	-0.5		
	55→58	-0.4		
5. [ $B_{3g}$ ]	55→58	-0.8	3.72	0.53
6. [ $A_g$ ]	57→60	-0.9	3.73	0.00
7. [ $B_{1u}$ ]	54→58	-0.8	4.21	1.77
	56→58	0.4		
8. [ $B_{3g}$ ]	56→60	0.7	4.28	0.00
	57→61	0.6		
	55→59	-0.9		
9. [ $A_g$ ]	55→59	-0.9	4.46	0.13
10. [ $B_{2u}$ ]	54→59	-0.9	4.56	0.55

trans tautomer are nearly the same as in siroberyllium. However, in the cis tautomer the HOMO  $b_1$  orbital has been destabilized and the LUMO  $b_1$  orbital has been stabilized. This leads to a decreased energy gap between the four orbital excitations involved in the  $Q$  and  $B$  states for the cis tautomer. Examining the molecular orbital coefficients of the  $b$  orbitals affected by this perturbation shows destabilization of the HOMO  $b_1$  due to a distortion of the positive charge towards the two nitrogens having a lower electron density (as determined by the relative size of the MO coefficients on the nitrogens) and stabilization of the LUMO  $b_1$  due to the distortion of the positive charge towards the two nitrogens having a higher electron density (larger MO coefficients). This seems to be the primary effect in causing the red shift of the cis tautomer relative to the trans.

There are some differences in the configurations contributing to the  $Q$  and  $B$  (Soret) states in the two sirohydrochlorin tautomers. There are two major configurations contributing to each of the  $Q$  and  $B$  states of the cis tautomer as predicted from the four orbital model. However, only one configuration is important in describing both  $Q$  states and one of the  $B$  (Soret) states in the trans tautomer. There is also a reversal of the main contributor to the highest  $Q$  state and the lowest  $B$  state between the two tautomers. The major configurations are noted in the table of predicted transitions (see Table 2).

**Table 5.** Orbital numbers, symmetries and energies for the porphine isomers<sup>b</sup>

Orbital number	Symmetry <sup>a</sup> cis trans	Cis orbital energies (eV)	Trans orbital energies (eV)
48	$a_1$ $b_{2u}$	-10.06	-10.14
49	$b_1$ $b_{2g}$	-10.05	-10.04
50	$a_2$ $a_g$	-9.93	-9.99
51	$a_2$ $b_{3u}$	-9.70	-9.97
52	$b_2$ $b_{1g}$	-9.62	-9.92
53	$b_1$ $b_{2g}$	-9.61	-9.53
54	$b_1$ $b_{3u}$	-9.01	-8.96
55	$a_2$ $b_{1g}$	-8.86	-8.83
56	$b_1$ $b_{3u}$	-6.90	-7.00
57 HOMO	$a_2$ $a_u$	-6.61	-6.47
58 LUMO	$b_1$ $b_{2g}$	-1.75	-1.61
59	$a_2$ $b_{1g}$	-0.57	-1.53
60	$b_1$ $a_u$	0.11	0.15
61	$a_2$ $b_{3u}$	0.77	1.06
62	$b_1$ $b_{2g}$	1.53	1.66
63	$a_2$ $b_{1g}$	1.64	1.81
64	$a_2$ $a_u$	2.05	2.03
65	$a_1$ $b_{3g}$	2.10	2.72
66	$b_1$ $a_g$	2.29	2.77
67	$a_1$ $b_{2u}$	2.38	2.78

<sup>a</sup> Symmetry designations follow Mulliken convention with axes oriented as in Figs. 3 and 4

<sup>b</sup> Cis isomer at  $C_{2v}$  MINDO/3 optimal geometry; trans isomer at the  $D_{2h}$  averaged X-ray geometry

Again, as a comparison we calculated the spectra of the porphine isomers using the averaged X-ray geometry for the trans and the MINDO/3 optimal  $C_{2v}$  geometry for the cis isomer. Tables 4 and 5 give the INDO/S/CI predicted transitions, orbital symmetries and energies. It should be noted that the symmetry labels for the cis porphine molecular orbitals and excited states are not exact because the wavefunction displays a first order symmetry instability, i.e. although the geometry has  $C_{2v}$  symmetry the wavefunction does not. Also, although the trans porphine bond orders indicate a  $D_{2h}$  wavefunction, the molecular orbitals do not have the symmetry of the irreducible representations of the point group. This orbital symmetry breaking allows mixing of configurations of "different" symmetry. For example, excited states 4 and 5 involve the mixing of the four orbital excitations which are nominally of  $B_{2u}$  symmetry with an excitation which is mostly of  $B_{3g}$  symmetry.

The porphine spectra predicted from INDO/S/CI are shown along with the locations of the experimental assignments in Fig. 9. The surprising feature of the calculation is the similarity of the cis and trans porphine isomers. Both show weak  $Q$  bands split by 0.3 and 0.4 eV. The splitting of the intense Soret bands is smaller for the cis (0.06 eV) than for the trans (0.19 eV). The INDO/S/CI calculation, unlike an earlier Pariser-Parr-Pople study [16], correctly shows no intense band between the Soret and the  $Q$  bands. It is difficult to say whether the cis or trans predicted transitions better fit the experimental data: While the relative intensity ratio of the two  $Q$  bands is fit by the trans, the absolute intensity is better fit by the cis. The experimental splitting of the Soret bands is somewhat ambiguous. It should be noted that the  $Q$  bands are predicted 0.5 to 0.7 eV too low in energy and the Soret bands 0.5 to 0.7 eV too high relative to the experimental assignments.

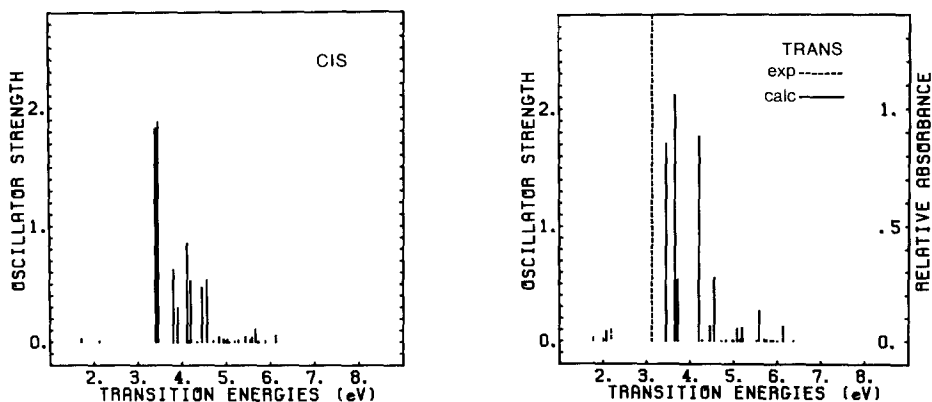


Fig. 9. Calculated transitions for the cis and trans porphine isomers and relative absorbances from the experimental spectrum of porphine. The experimental spectrum is believed to result only from the trans tautomer

## Summary

Although we encountered difficulties in trying to compare the ground state energies and electronic transitions for the *cis* and *trans* isomers of these free base porphyrins due to symmetry instability problems, the calculations clearly predict the *cis* form of sirohydrochlorin to be close in energy to the *trans* with a red shifted spectrum. Our excited state calculations confirm Chang's identification of the *cis* and *trans* sirohydrochlorin as the "red" and "orange" tautomers, respectively. The calculations on the porphine isomers have provided a reference and these clearly show that the *trans* porphine isomer is the more stable than the *cis*, as expected experimentally. However, the spectra calculated for the two porphine isomers are surprisingly similar and difficult to distinguish.

*Acknowledgement.* We thank Dr. C. K. Chang of Michigan State University and Dr. Jack Fajer of Brookhaven National Laboratory for pre-publication data on sirohydrochlorin. Dr. Michael Zerner of the University of Guelph and Dr. Gilda Loew of SRI International kindly provided the INDO program. This work was supported by NSF grant DMR-7823958 and NIH grant GM22937-06.

## References

1. Battersby, A. R., Jones, K., McDonald, E., Robinson, J. A., Morris, H. R.: *Tetrahedron Lett.* **2213** (1977)
2. Deeg, R., Kriemler, H. P., Bergmann, K. H., Muller, G.: *Hoppe-Seylers Z. Physiol. Chem.* **358**, 339 (1977)
3. Scott, A. I., Irwin, A. J., Siegel, L. M., Shooley, J. N.: *J. Am. Chem. Soc.* **100**, 7987 (1978)
4. Murphy, M. J., Siegel, L. M., Kamin, H., Rosenthal, D.: *J. Biol. Chem.* **248**, 2801 (1973);  
Murphy, M. J., Siegel, L. M., Tove, S. R., Kamin, H.: *Proc. Natl. Acad. Sci. USA* **71**, 612 (1974)
5. Vega, J. M., Garrett, R. H., Siegel, L. M.: *J. Biol. Chem.* **250**, 7890 (1975)
6. Chang, Chi K.: *Biochemistry* **19**, 1971 (1980); Antipas, A., Chang, C. K., Gouterman, M., Merriam, T. S., Williams, L. D., unpublished
7. Gouterman, M.: *J. Mol. Spectrosc.* **6**, 138 (1961); Gouterman, M., Wagniere, G. H., Snyder, L. C.: *J. Mol. Spectrosc.* **11**, 108 (1963)
8. Bingham, Richard C., Dewar, M. J. S., Lo, D. H.: *J. Am. Chem. Soc.* **97**, 1285 (1975)
9. Barkigia, K. M., Fajer, J., Chang, C. K., Williams, G. J. B.: *J. Am. Chem. Soc.* **104**, 315 (1982)
10. Chen, Betty M. L., Tulinsky, A.: *J. Am. Chem. Soc.* **94**, 4144 (1972)
11. Storm, C. B., Teklu, Y.: *J. Am. Chem. Soc.* **94**, 1745 (1972)
12. Barkigia, K. M., Fajer, J., Spaulding, L. D., Williams, G. J. B.: *J. Am. Chem. Soc.* **103**, 176 (1981)
13. Baumann, H.: *J. Am. Chem. Soc.* **100**, 7196 (1978)
14. Dewar, M. J., Haddon, R. C., Student, P. J.: *J. Chem. Soc., Chem. Commun.* 569 (1974)
15. Zerner, M., Ridley, J.: *Theoret. Chim. Acta (Berl.)* **32**, 111 (1973)
16. McHugh, A. J., Gouterman, M.: *Theoret. Chim. Acta (Berl.)* **24**, 346 (1972)

Received November 9, 1981